DIFFRACTIVE FINAL STATES AT H1

B. M. WAUGH
FOR THE H1 COLLABORATION
Department of Physics and Astronomy, The University of Manchester, UK

The hadronic final state in diffractive deep-inelastic e^+p scattering is studied using energy flow, charged particle spectra, multiplicity of charged particles, and thrust The results are compared with data from other processes and with Monte Carlo predictions. Clear evidence is found for a significant contribution from processes in which the exchanged photon interacts with a gluon.

1 Introduction

The measured diffractive structure function $F_2^{D(3)}$ is found to be consistent with a model in which diffractive deep-inelastic scattering (DDIS) is due to the exchange of a pomeron ($I\!P$) with a partonic structure dominated by hard gluons [1]. Complementary tests of the mechanism underlying DDIS are provided by studies of the hadronic final state [2,3,4], as described in this talk. In particular, the results are discussed in terms of the partonic content of the pomeron. A quark-dominated pomeron would lead predominantly to an aligned-jet configuration from the hadronization of a $q\bar{q}$ partonic final state, with final-state hadrons concentrated close to the $\gamma^* I\!P$ axis in the centre-of-mass frame (CMS) of the $\gamma^* I\!P$ system. A gluon-dominated pomeron gives rise to a significant fraction of events with less alignment and a larger parton multiplicity ($q\bar{q}g$ etc.) and hence to more energy flow away from the $\gamma^* I\!P$ axis, more transverse momentum relative to this axis, and lower thrust. The fragmentation of the more complex system of colour strings in a gluon-initiated process also adds to the energy flow in the central region and leads to a larger hadron multiplicity.

The data are compared with predictions from the RAPGAP 2.02 [5] generator using two different partonic structures for the pomeron: RG–F_2^D (fit 3) has a hard gluon distribution; RG–F_2^D (fit 1) has a distribution including only quarks at low Q^2. Both pomeron structures are taken from fits [1] to $F_2^{D(3)}$. Also shown are predictions from LEPTO 6.5 [6], which generates diffractive events using a soft colour interaction (SCI) model.

2 Results

All analyses described here are carried out in the CMS of the $\gamma^* I\!P$ system.

Figure 1(a) shows the energy flow [2] against pseudorapidity η^* in three regions of M_X. The distribution is approximately symmetrical about $\eta^* = 0$ and

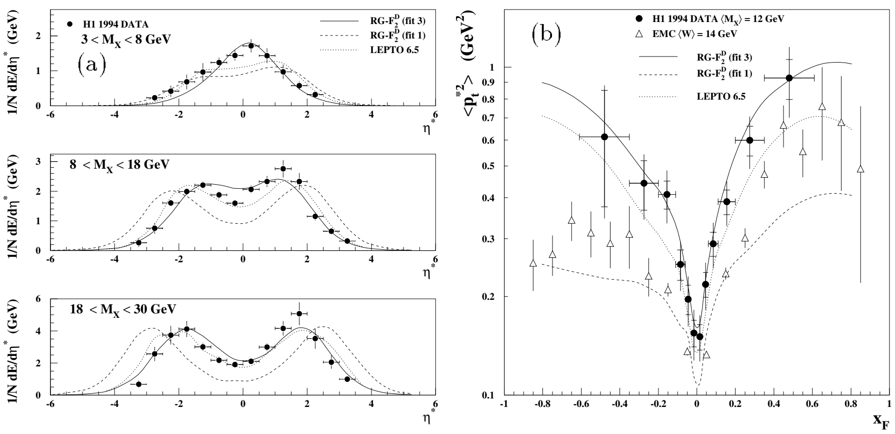

Figure 1: (a) Energy flow vs pseudorapidity in three regions in M_X. The pseudorapidity is $\eta^* = \log(\tan(\theta^*/2))$, where θ^* is the polar angle with respect to the direction of motion of the incoming photon. Thus positive η^* corresponds to the current and negative η^* to the target region. Also shown are predictions from RAPGAP and LEPTO. (b) Seagull plot: $\langle p_T^{*2} \rangle$ vs x_F. The Feynman variable is defined as $x_F = 2 \cdot p_{\|}^*/M_X$, where $p_{\|}^*$ is the component of a particle's momentum along the direction of motion of the incoming photon. Thus positive x_F corresponds to the current and negative x_F to the target region. Also shown are data on non-diffractive DIS from EMC; in this case the $\gamma^* p$ CMS is used and M_X is replaced by the $\gamma^* p$ invariant mass W in the definition of x_F. Also plotted are predictions from RAPGAP and LEPTO.

shows a double-peaked structure becoming more pronounced with increasing M_X. This appearance is compatible with a final state consisting primarily of a two-jet system, with a preference for being aligned with the $\gamma^* I\!P$ axis. However, the RG–$\mathrm{F}_2^{\mathrm{D}}$ (fit 1) model predicts too much alignment and is incompatible with the larger observed energy flow in the central region. The RG–$\mathrm{F}_2^{\mathrm{D}}$ (fit 3) model predicts more energy in the central region and provides a better description of the data. LEPTO also describes the data fairly well for $M_X > 8\,\mathrm{GeV}$.

Figure 1(b) shows the "seagull plot" [2]: the mean squared transverse momentum of charged particles plotted against the Feynman variable x_F. The mean p_T^2 is higher in DDIS than in non-diffractive DIS over a wide range, indicating a larger gluon content in the pomeron than in the proton. The final state in DDIS is approximately symmetrical about $x_F = 0$. This contrasts with the data from non-diffractive DIS, which show a suppression of high-p_T parton radiation from the extended proton remnant in the target region.

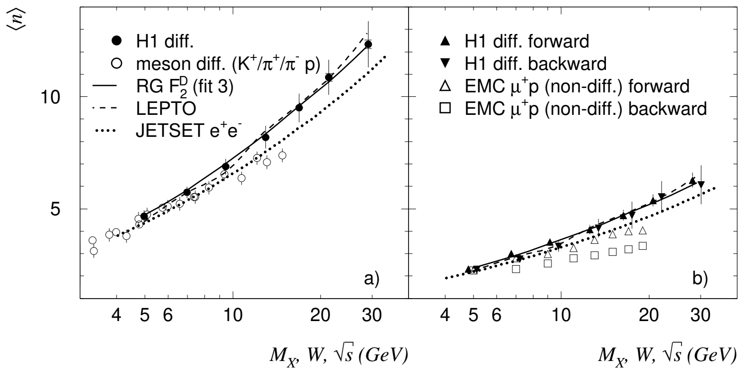

Figure 2: (a) Mean multiplicity of charged particles plotted against M_X. Also shown are data on meson diffraction, predictions from JETSET (which is known to reproduce well the results for e^+e^- scattering) and predictions from RAPGAP and LEPTO. (b) Mean multiplicity in the current (forward) and target (backward) hemispheres separately. Also shown are results from non-diffractive DIS at EMC.

Figure 2(a) shows the mean number of charged particles [3] as a function of M_X. The multiplicities for DDIS, meson diffraction and e^+e^- scattering are similar at low masses, but for $M_X \gtrsim 10\,\mathrm{GeV}$, the multiplicity grows faster with mass in DDIS than in the other processes. This points to a larger contribution in DDIS from higher parton multiplicities. The final states in meson diffraction and e^+e^- scattering are both expected to be dominated by the simpler $q\bar{q}$ system. The RG–$\mathrm{F}_2^{\mathrm{D}}$ (fit 3) and LEPTO models describe the data fairly well. Figure 2(b) shows the data in the forward and backward hemispheres separately. Again, the symmetry of the final state in DDIS contrasts with the asymmetry in non-diffractive DIS.

The thrust T provides a measure of the "elongation" of the event; it is defined more rigorously elsewhere [4]. Figure 3 shows the mean thrust [4] $\langle T \rangle$ as a function of $1/M_X$. The value of $\langle T \rangle$ is lower in DDIS than in e^+e^- scattering. This indicates that the final state in diffractive DIS is less collimated than that in e^+e^-, where the topology is dominated by the simple $q\bar{q}$ two-jet system. This is consistent with a larger contribution from higher parton multiplicities ($q\bar{q}g$ etc.). The RG-q$\bar{\mathrm{q}}$ model predicts too high a value of $\langle T \rangle$; RG–$\mathrm{F}_2^{\mathrm{D}}$ (fit 3) and LEPTO are closer to the data.

3 Summary and Conclusions

Measurements of the hadronic final state in diffractive deep-inelastic scattering indicate a significant contribution from processes involving a gluon in the hard

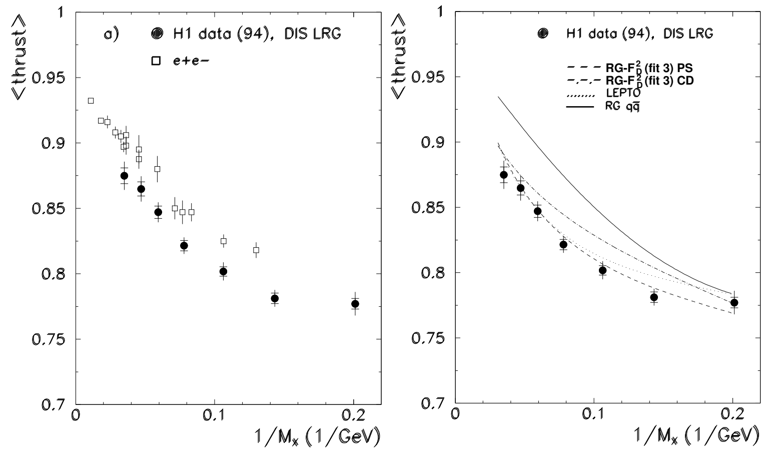

Figure 3: (a) Mean thrust vs $1/M_X$, compared to data from e^+e^- interactions; (b) The same data compared to RAPGAP and LEPTO. Two different schemes were used to handle higher-order QCD effects in RAPGAP: parton showering (PS), and colour dipole fragmentation (CD).

subprocess. A model in which the pomeron has a partonic structure dominated by hard gluons provides a reasonable description of the data, whereas a pomeron with only quarks at low Q^2 leads to too little energy flow in the central region, too little transverse momentum, too few charged particles and too high a value of the thrust. A model based on soft colour interactions (SCI) also describes the data reasonably well.

Acknowledgments

Thanks to all those who contributed to the analyses presented here.

References

1. H1 Collaboration, *Z. Phys.* C76 (1997) 613.
2. H1 Collaboration, DESY preprint 98–029, accepted by *Phys. Lett.* B.
3. H1 Collaboration, DESY preprint 98–044, submitted to *Eur. Phys. J.*
4. H1 Collaboration, *Eur. Phys. J.* C1 (1998) 495.
5. H. Jung, *Comp. Phys. Comm.* 86 (1995) 147;
   H. Jung, *RAPGAP 2.02 Program Manual*, 1996 (unpublished).
6. G. Ingelman et al., *Comp. Phys. Comm.* 101 (1997) 108.